The role of Glu^{498} in the dioxygen reactivity of CotA-laccase from *Bacillus subtilis*

Zhenjia Chen[*], Paulo Durão[*], Catarina S. Silva[*], Manuela M. Pereira[*], Smilja Todorovic[*], Peter Hildebrandt[†], Isabel Bento[*], Peter F. Lindley[*,‡] and Lígia O. Martins[*]

[*]*Instituto de Tecnologia Química e Biológica, Universidade Nova de Lisboa, Av. da República, 2781-901 Oeiras, Portugal.*

[†]*Technische Universität Berlin, Institut für Chemie, Sekr. PC 14, Straße des 17. Juni 135, D-10623 Berlin, Germany.*

[‡]*Department of Crystallography, Birkbeck College, University of London, Malet St., London WC1E 7HX, United Kingdom.*

Running title: Mutations at the laccase trinuclear Cu site
Key words: laccase, multicopper oxidase, dioxygen reduction, trinuclear Cu centre, site-directed mutagenesis, CotA laccase

Corresponding Authors: lmartins@itqb.unl.pt Tel: +351 214469534, Fax: +351 214411277, bento@itqb.unl.pt Tel : +351 214469662, Fax : +351 214433644

ABSTRACT

The multicopper oxidases couple the 1-electron oxidation of four substrate molecules to the four electron reductive cleavage of the O-O bond of dioxygen. In this study, the role of the Glu^{498} residue, located within the entrance channel to the trinuclear copper centre, has been investigated in binding and reduction of dioxygen by the CotA-laccase from *Bacillus subtilis*. The replacement of this glutamate by aspartate, allows the enzyme to retain its catalytic activity at levels close to those exhibited by wild-type. The absence of an acidic group at the 498 residue, as in the E498L and E498T mutants, results in severe catalytic impairment, 0.7% and 0.04%, respectively, relative to that of the wild-type. Furthermore, the latter mutants show increased K_m values for dioxygen, while the E498D mutant shows a similar affinity constant to that of the wild-type protein. X-ray structural and spectroscopic analysis (UV-visible, electron paramagnetic resonance and resonance Raman) reveal perturbations of the structural properties of the catalytic centres in the Glu^{498} mutants when compared to the wild-type protein. Overall, the results strongly suggest that Glu^{498} plays a key role in the stabilization of the trinuclear centre, controlling the binding of dioxygen and its further reduction.

INTRODUCTION

CotA-laccase is a structural component of the outer layer of the spore coat from *Bacillus subtilis* [1], and is thought to be involved in the synthesis of the brown pigment that protects the spore against UV light. Similarly to all the members of the multi-copper oxidase (MCO) family, it is able to couple one-electron oxidation of four substrate equivalents with the four-electron reduction of dioxygen to water [2-5]. The catalytic motif in these enzymes includes three distinct copper centres [6]. Type 1 (T1) Cu is characterized by an intense $S(\pi) \rightarrow Cu(d_{x^2-y^2})$ charge transfer (CT) absorption band at around 600 nm, responsible for the intense blue colour of these enzymes, and a narrow parallel hyperfine splitting [$A_{\parallel}$ = (43-90) x 10^{-4} cm^{-1}] in the electron paramagnetic resonance (EPR) spectra. This is the site of substrate oxidation and in this respect the MCO family can be separated into two classes; enzymes that oxidize small organic substrates with high efficiency and those that oxidize metal ion substrates [5]. The trinuclear centre, where dioxygen is reduced to water, comprises two type 3 (T3) and one type 2 (T2) copper ions. The two T3 Cu ions, which are usually antiferromagnetically coupled through a bridging ligand and therefore EPR silent, show a characteristic absorption band at 330 nm. The T2 Cu copper site lacks strong absorption bands but exhibits a large parallel hyperfine splitting in the EPR spectra [$A_{\parallel}$ = (150-201) x 10^{-4} cm^{-1}].

CotA-laccase is able to oxidise a variety of substrates including non-phenolic and phenolic compounds, and also a range of synthetic azo and anthraquinonic dyes, thus having a potential use for diverse biotechnological applications [7-9]. Several structure-function relationship studies have been performed with this enzyme [10-13]. They revealed redox properties of the T1 copper site and gave structural insights into the principal stages of the mechanism of dioxygen reduction at the trinuclear centre. Electrons from the reducing substrate are supplied to the MCOs through the T1 Cu site and then transferred over a highly conserved Cys-His electron-transfer pathway to the T2/T3 cluster. Two reaction intermediates have been identified during dioxygen reactions of MCOs [14-18]. Intermediate I, or a peroxide intermediate, accounts for a two-electron reduced form of dioxygen. The other reaction intermediate II, or the "native intermediate", has been detected at the final stage of a single catalytic turnover, after the transfer of four electrons to dioxygen. Careful comparison of crystal structures shows that MCOs have, with very rare exceptions, conserved negatively charged residues close to the trinuclear site, a glutamate within the entry channel for dioxygen, and an aspartate in the exit channels of the trinuclear centre [10, 19-28]. These residues may facilitate binding of dioxygen and supply of protons to the reaction intermediate as suggested by mutagenesis studies performed with a few multicopper oxidases [29-33]. A crucial role of Glu^{498} has been suggested in channelling protons needed for dioxygen reduction in CotA-laccase based on structural and modelling data (unpublished results). In the present work, the importance of Glu^{498} (Figure 1) has been examined in the mechanism of dioxygen reduction by replacing this residue by aspartate, threonine and leucine. A combination of enzyme kinetic measurements, spectroscopic techniques and structure determination by X-ray crystallography showed that this acidic residue is involved in channelling of protons to the trinuclear centre, but also has a role in stabilisation of this catalytic centre.

MATERIAL AND METHODS

Construction of CotA mutants. Single amino acid substitutions in the trinuclear centre were created using the QuickChange site-directed mutagenesis kit (Stratagene). Plasmid pLOM10 (containing the wild-type *cotA* sequence) was used as a template [1] and the primers forward 5'-

TGC CAT ATT CTA GAG CAT TTA GAC TAT GAC ATG – 3' and reverse 5'- CAT GTC ATA GTC TAA ATG CTC TAG AAT ATG GCA -3' were used to generate the E498L. The primers forward 5'- TGC CAT ATT CTA GAG CAT ACA GAC TAT G-3' and reverse 5'- CAT AGT CTG TAT GCT CTA GAA TAT GGC A-3' were used to generate the E498T mutation. At last, the primers forward 5´- TGC CAT ATT CTA GAG CAT GAT GAC TAT G-3' and reverse 5'- CAT AGT CAT CAT GCT CTA GAA TAT GGC A-3' were used to generate the E498D mutant. The presence of the desired mutations in the resulting plasmids (pLOM53 (carrying the E498L point mutation), pLOM54 (bearing the E498T point mutation), and pLOM56 (with the E498D mutation) and the absence of unwanted mutations in other regions of the insert were confirmed by DNA sequence analysis. Plasmids pLOM53, pLOM54 and pLOM56 were transformed into *Escherichia coli* Tuner (DE3) strains (Novagen) to obtain strains LOM408, LOM413 and LOM417, respectively.

Overproduction and purification. Strains AH3517 (containing pLOM10), LOM408, LOM413 and LOM417 were grown in Luria–Bertani medium supplemented with ampicillin (100 µg/mL) at 30ºC. Growth was performed as described by Durão *et al.* [34] according to the optimized protocol to yield a protein population fully-loaded with copper. Cell harvesting and disruption and subsequent purification of proteins by using a two-step protocol procedure were performed as previously described [1,10]. Purified enzymes were stored at -20ºC until use.

UV–visible, EPR and RR Spectroscopy. UV–visible spectra were acquired using a Nicolet Evolution 300 spectrophotometer from Thermo Industries. EPR spectra were measured with a Bruker EMX spectrometer equipped with Oxford Instruments ESR-900 continuous-flow helium cryostat, with a microwave frequency of 9.39 GHz, power of 2.0 mW and modulation amplitude of 0.9 mT. The spectra obtained under non-saturating conditions (100 to 160 μM protein contents) were theoretically simulated using the Aasa and Väangard approach [35]. RR spectra of 1mM CotA wild-type, 2 mM E498T, 1.5 mM E498D and 0.8 mM E498L mutants (in 20 mM Tris buffer, pH 7.6) were measured as described before [12], with 568 nm excitation, at -190°C.

Redox titrations and enzyme assays. Redox titrations were performed at 25 ºC in 20 mM Tris-HCl buffer pH 7.6 containing 0.2 mM NaCl under an argon atmosphere, and were monitored by visible spectroscopy (300–900 nm), using a Shimadzu Multispec-1501 spectrophotometer, as previously described by Durão et al.[11]. The laccase-catalysed oxidation of ABTS and 2,6-dimethoxyphenol (2,6-DMP) were photometrically monitored at 37°C in air saturated conditions by using the methods described by Durão et al. [11]. Activities were also performed following the rate of oxygen consumption varying the concentrations of dioxygen at fixed concentration of the reducing substrates (ABTS or 2,6-DMP) by using an oxygen electrode (Oxygraph; Hansatech, Cambridge UK). Stock solutions of 10 mM of ABTS (pH 4) and 50 mM 2,6-DMP (pH 7 or pH 5.6) were prepared in Britton Robinson buffer. The oxygen electrode was calibrated at 37ºC using buffer saturated with air and buffer deoxygenated with sodium dithionite. The initial concentration of dioxygen in solution was controlled by flushing the reaction vessel with a mixture of nitrogen and oxygen with the aid of two flowmeters. All the reactions were corrected for background autoxidation. The kinetic constants K_m and k_{cat} were fitted to the Michaelis-Menten model (Origin-Lab, Northampton, MA, USA). All enzymatic assays were performed at least in triplicate. The protein concentration was measured by using the absorption band at 280 nm (ε_{280}=84,739 M^{-1} cm^{-1}) or the Bradford assay using bovine serum albumin as a standard [36].

Azide inhibition. Enzymes were incubated with sodium azide (0 to 100 mM, final concentration) for different periods of time (0, 30, 60, 120 min) followed by activity measurements towards

ABTS oxidation (1mM) with wild-type (0.0001 mg/ml) and mutant enzymes (0.02 to 2 mg/ml) in Britton-Robinson buffer at the optimum pH value.

Crystallization. Crystals of the CotA mutant proteins were obtained by the vapour diffusion method, at room temperature, from crystallisation media containing 8-10% of PEG 4K, 26-30% of isopropanol and 0.1 M of sodium citrate pH 5.5. The crystals were harvested and cryo-frozen with a solution that contained the crystallisation medium plus 22% of ethylene glycol.

X-ray data collection and refinement. X-ray diffraction data were collected at 110 K using the macromolecular crystallography beam lines as indicated in Table 1, at the European Synchrotron Radiation Facility at Grenoble, France. Data sets were processed and scaled using MOSFLM [37] and SCALA from the CCP4 program suite [38]. The structure solution for each CotA mutant was found by the molecular replacement method, using the MOLREP program [39]. The structure of CotA (PDB code: 1W6L) [10] from which all the copper atoms and solvent molecules were removed served as a search model. For each mutant a unique solution was determined; typical R-factors and scores were 0.40 and 0.74 respectively. Refinement was performed using the maximum likelihood functions in the REFMAC program [40], while model building and improvement were achieved with COOT [41]. Solvent molecules were positioned after a few cycles of refinement as well as several molecules of ethylene glycol. Isotropic refinement of the atomic displacement parameter was performed for all atoms. The occupancies of the copper ions were adjusted so that their isotropic thermal vibration parameters refined approximately to those observed for the neighbouring atoms. The careful use of omit and standard difference Fourier syntheses, as well as monitoring of thermal vibration coefficients during refinement, enabled the identification of a diatomic species placed in between the type 3 copper sites in all three mutants. These species were assumed to be a dioxygen type species and refinement proceeded constraining the O-O distances to target values of 1.08 Å. Similarly to what has been observed for the native fully loaded CotA, additional electron density was observed close to the Cys 35 and this was modelled as an oxidised cysteine residue in two of the three mutants. In the E498T mutant two alternate conformations were modelled for the side chain of the OXY-Cys 35, whereas in the E498L mutant a mixture of Oxy-Cys and Cys was modelled according to the electron density map. In the E498D mutant no alteration was observed and a cysteine side-chain was modelled in two alternate positions. As observed in the other crystals structures of CotA, the loop comprising residues 89 to 97 was poorly defined in the electron density maps in all three mutants and was not modelled. The final statistics of the refinement procedure are listed in Table S1 in the Supplementary material.

RESULTS

Kinetic characterization of mutant enzymes

Site-directed replacement of Glu^{498} by leucine, threonine and aspartate resulted in enzymes that show the same chromatographic pattern during purification when compared to the wild-type CotA-laccase. Metal analysis indicated that all “as isolated” proteins contained around 4 moles of copper ions per mol of protein (with an associated 15% error, Table 2S, Supplementary Material). Two reducing substrates, one non-phenolic (ABTS) and one phenolic (2,6-DMP), were used to identify specific changes in the catalytic properties of the studied mutant proteins. The optimum pH value for the oxidation of both substrates is in the case of E498L and E498D similar to the wild-type, while E498T mutant displays a 1.6 unit decrease for the oxidation of 2,6-DMP (Figure 2). A comparison of the catalytic activities at the optimum pH shows that mutations in the Glu^{498}

residue result in a lower catalytic efficiency when compared with the wild-type CotA (Table 2). Mutant E498L is the most affected in this respect showing virtually no enzymatic activity, with 3 to 4-orders of magnitude decreased efficiency (k_{cat}/K_m). The E498T mutant shows 2 to 3-orders of magnitude lower efficiency in relation to wild-type. On the other hand, the E498D mutant shows catalytic efficiency closest to that of the wild-type strain, with a decrease between 10 and 45 times, depending on the substrate. Considering that only half of the E498D protein population has fully loaded T1 site (see below), efficiency could be calculated as only 5 to 23 times lower than that of wild-type. Neither of the mutations resulted in major and consistent alterations of K_m for the tested substrates and thus lower efficiency values are mainly due to a decrease of k_{cat} values.

The Michaelis-Menten constants for dioxygen reactivity (K_m (O_2)) of wild-type and mutants at the optimal pH are shown in Table 3. The K_m (O_2) value measured for the wild-type and the E498D mutant was similar and, at the same time close to the values reported for other laccases [42 and references herein]. The mutants E498T and E498L exhibited around 2 to 4-fold lower values, respectively, suggesting a different binding interaction with O_2 in the steady state. The use of ABTS or 2,6-DMP as the reducing substrate did not significantly affect the K_m (O_2) (data not shown). The k_{cat} (O_2) values are similar to the k_{cat} (ABTS) or k_{cat} (2,6-DMP) (Table 2), as anticipated for a steady state with efficient coupling of the two redox halves of the catalysis. The ability of the trinuclear cluster to bind molecular oxygen, and to retain its partially reduced forms during the catalytic cycle is reflected in the relatively high affinity of this site for a number of anions [4]. Azide is one of the most studied laccase inhibitors and in the CotA-laccase crystal structure soaked with azide, this molecule bridges the type 3 copper ions [10]. The inhibition of CotA and Glu^{498} mutants was followed in the presence of increasing concentrations of sodium azide. Total inhibition was observed at a concentration of 80 mM sodium azide, after a preincubation period of 30 min. For the wild-type enzyme and E498D mutant similar I_{50} values (concentration of inhibitor required for achieving 50% reduction of the activity) were measured, while the E498T and E498L mutants show 2 and 4-fold higher I_{50} values as compared with CotA-laccase (Table 3).

Spectroscopic characterization of Glu^{498} mutants

The UV-visible absorption spectrum of wild-type CotA is dominated by two intense charge transfer (CT) bands; a band centred at 609 nm originating from the T1 site and a shoulder at 330 nm associated with the T3 site, both with ε values around 4,000 M^{-1} cm^{-1} (Figure 3 and Table S2, in the Supplementary material). All mutants in their as-isolated state appear to be partially reduced, as after treatment with potassium iridate an increase of both intensity absorption bands was observed. Nevertheless, after the oxidation step, the maximal absorption intensity at 609 nm was lower than in the wild-type, by 55% for E498D, 27% for E498T and 10% for E498L, suggesting some T1 copper depletion in all mutant proteins. Mutants E498T and E498D seem to be fully reactive with dioxygen, since transition bands at 609 and 330 nm, rapidly recover after exposure to air, from dithionite-reduced proteins, in a similar manner as observed for the wild-type enzyme. However, the mutant E498L remained in the reduced state even after being exposed to the air for 24h, revealing highly impaired reactivity towards dioxygen.

The S(Cys)-Cu vibrational modes of T1 site are selectively enhanced in RR spectra obtained by excitation into $S(\pi)\rightarrow Cu(d_{x^2-y^2})$ CT [4]. The spectra of the wild type, E498T and E498D mutants show several vibrational modes with stretching character centred at 400 cm^{-1}, with some subtle differences (Figure S1 in the Supplementary material). The most intense band, which appears to have the greatest Cu-S(Cys) stretching character, is downshifted from 425 cm^{-1} to 417 cm^{-1} in the

E498L mutant. However, the intensity weighted frequency of all stretching coordinates for all mutant proteins (409 cm^{-1}) is very similar to that of the wild type (410 cm^{-1}), revealing an absence of substantial differences on the level of electronic configuration of the T1 site [12]. Moreover, the S/N ratio is much lower in the spectrum of E498D, under the same experimental conditions and comparable protein concentration, evidence that this mutation decreased the stability of the T1 site. All mutants present similar redox potentials of the T1 Cu site of the wild-type enzyme (525 mV, Table S2 in the Supplementary material).

The EPR spectra show strong similarities between wild-type CotA and E498L mutant, while the E498T and E498D mutants spectra show remarkable differences (Figure 4). Spectral deconvolution (data not shown) revealed that the copper T1 site in the latter mutants has the same conformation as in the wild-type protein, since it was simulated using the same spin Hamiltonian parameters (Table 4). However, for the E498D mutant, depletion in T1 site has been observed as revealed by spectral integration, indicating that only half of the E498D population contains copper at this site. Nonetheless, the EPR spectra reveal the most striking differences between the mutants at the T2 copper site. In the case of E498T, the g_{max} for this centre is higher than in the wild-type, while the hyperfine constant is lower, indicating that the copper T2 site in this mutant has a different conformation or experiences a different electronic vicinity (named the T2' form). Interestingly, both forms of the type 2 Cu, the one observed for the wild-type and E498L (T2) and that of E498T (T2'), are present in the E498D mutant. This protein spectrum can be simulated using the parameters of the T2 and T2' forms, integrated in a 1:1 ratio. A careful inspection of the EPR spectrum of the wild-type CotA reveals the presence of a very small signal identical to that assigned to the T2' form (Figure 4).

Structural details of the mutant enzymes

The overall structure of the Glu^{498} mutant CotA proteins is essentially the same as the one obtained for the wild-type enzyme. Superposition of the backbones of each of the mutants onto the fully-copper loaded CotA structure [38] gives root mean square deviations of only 0.131Å, 0.124Å and 0.131Å for E498D, E498L and E498T mutants, respectively. The observed differences are located at the copper centres and in their neighbourhood. In the E498D mutant the orientation of the side chain of the mutated aspartate is different from the one observed for the native glutamate residue. In the native CotA-laccase the glutamate is pointing towards the solvent channel, making a H-bond with a water molecule that interacts with the dioxygen moiety found in between the two T3 copper ions (Figure 5A). In the E498D mutant, the aspartate points towards the interior of the protein having its $O^{\delta 1}$ atom at a H-bond distance from $N^{\delta 1}$ atom of His^{491} (Figure 5B). In this mutant, the water molecule interacting with the dioxygen moiety in the native structure no longer exists. Moreover, all copper atoms in the trinuclear centre are fully occupied, as observed in the wild-type enzyme (Table S3 in the Supplementary material). However, the occupancy of the T1 copper site in E498D is significantly less than one (0.7), corroborating the UV-Vis, RR and EPR data, although at first sight there appears to be no obvious structural reason for this finding. In the E498T mutant containing a polar residue with a shorter side-chain than the native glutamate, no difference was found in copper occupancy in the type 1 copper centre, but a decrease of occupancy to 0.8 was observed for all the copper ions in the tri-nuclear centre (Figure 5C). The same was observed for the E498L mutant (Figure 5D). This effect was even more pronounced for the type 2 copper ion, which refined to an occupancy of only 0.3. In all three mutants a dioxygen moiety was modelled in between the two type 3

copper ions and refined with the same occupancy that was observed for the type 3 copper ions (Figure 5).

DISCUSSION

This study aimed to address the role of residue Glu^{498}, found in the second coordination sphere of the trinuclear centre of CotA-laccase. Three mutant enzymes were designed and expressed and the resulting proteins purified. Their catalytic properties were determined, and furthermore their structural differences were addressed by spectroscopic techniques and X-ray crystallography. All MCO appear to have an acidic residue (Glu^{498} in CotA) accessible to the entrance channel by which dioxygen reaches the trinuclear centre. This residue has been found to participate in the proton assisted reductive cleavage of the O-O bond at the trinuclear site in yeast Fet3p and CueO from *E. coli* [29, 43]. In the CotA laccase, the carboxylic moiety of Glu^{498} is hydrogen bonded to a water molecule which is further hydrogen bonded to the dioxygen moiety, almost symmetrically positioned in between the type 3 copper ions [10]. The mutation of Glu^{498} to a shorter aspartate residue aimed to change the spatial rearrangement of the water molecule, while eliminating the carboxylic moiety in the E498T and E498L mutants was designed to abolish the connectivity of this residue with the trinuclear Cu cluster. The E498D mutant mostly resembles the wild-type enzyme in terms of enzymatic activity towards both ABTS and 2,6-DMP substrates, as well as dioxygen-binding affinity and azide inhibition. The orientation of the side chain of the mutated aspartate is different from that observed for the native glutamate residue. However, kinetic data show that it is still able to maintain the H-bond network necessary for increased the electron affinity for dioxygen, peroxide intermediate formation and therefore to assist in the reductive cleavage of the O-O bond. A polar threonine side chain has very low proton donating ability while an apolar leucine side chain will not provide any protons under the normal reaction conditions. Accordingly, the E498L and E498T mutants, without a protonable species from this position, show a severe catalytic impairment. Several mutagenesis studies have shown the role of an additional conserved acidic residue (corresponding to Asp^{116} in CotA-laccase) located at the "outershpere" of the trinuclear centre, in channelling protons in the O-O bond cleavage process [29-33]. The carboxylic moiety of this aspartate residue, is hydrogen bonded to a water molecule which, in turn, is hydrogen bonded to the T2 hydroxide ligand, contributing to the hydrogen-bonding network of the trinuclear centre and thus to its stability and reactivity. The results of the present study indicate that protons from the bulk water, supplied through channels leading to the trinuclear centre [10], without the final assistance of Glu^{498}, are insufficient to provide the needed protons for the catalytic process. Moreover, these results also suggest the absence of alternative pathways participating in the transfer of protons to the trinuclear centre of CotA-laccase.

A perturbation of the T1 copper centre in the E498D mutant was observed by spectroscopic and crystallographic data. Different orientation of the aspartate residue, as compared to the wild type and E498T and E498L mutants, with its $O^{\delta 1}$ atom at a H-bond distance from the $N^{\delta 1}$ atom of His^{491}, is likely to cause destabilisation of the type 1 copper site, by opening this centre and promoting its depletion, as observed experimentally. In fact, His^{491} is coordinated to one of the two T3 copper ions in the tri-nuclear centre (Cu3) while the residue 498 is adjacent to His^{497} which coordinates directly to the type 1 copper atom. In the crystal structure of the E498D mutant no significant difference in the bond length between the His^{497} residue and the copper atom in the type 1 copper centre was observed. However, a 2 fold-lower K_m was measured in this mutant for the reducing substrate ABTS. This finding could be indicative of subtle alterations

near His^{497}, a residue most probably involved in ABTS binding and further electron transfer to the T1 Cu site of CotA-laccase [13].

The geometry of the trinuclear centre of Glu^{498} mutants is essentially the same as that found previously in the native structure (see for example [10]) except for the lower occupancy at T3 and T2 centres in the E498T and E498L mutants. However the EPR spectra of the E498L mutant are similar to those of wild-type in apparent contradiction with the X-ray results. It is possible that this discrepancy result from a destabilising effect of the mutation at the trinuclear centre making it more prone to loosing copper during crystallization. Some heterogeneity of the T2 species in E498D and E498T mutants are revealed in the EPR spectra. The nature of the "new" T2' form is not clear at this point. It can be due to direct structural (or conformational) alterations caused by the mutations or alternatively, it could result from an intermediate state stabilized by the mutations, scarcely detected in the wild-type protein. The existence of different forms of type 2 copper was also observed in the case of bilirubin oxidase where an aspartate residue close to that site has been mutated [30]. The partial reduction of the dioxygen moiety and/or the simultaneous presence of a hydroxyl and a water molecule bound to the T2 centre, in direction of the exit channel, could give rise to two types of centre. The resolution of the X-xay crystal data does not, however, permit any significant structural insights in the geometry of the T2 copper centre that would confirm the spectroscopic data. Nevertheless, there has to be some flexibility at this centre to allow the water molecules, formed by the reduction of dioxygen, to access the exit channel. The concomitant movement of the T2 copper may be reflected by the EPR data.

The results of this study unequivocally indicate that the electrostatic environment of the trinuclear centre of CotA-laccase is determined through the direct or indirect hydrogen bonding with Glu^{498}. These hydrogen bonds are highly conserved in the multicopper oxidases and are part of a large hydrogen-bonding network around the trinuclear Cu cluster that contributes to its reactivity and stability [14, 15]. The lack of reactivity of the E498L and E498T mutants towards dioxygen suggests that the hydrogen bond connectivity of the Glu^{498} plays an electronic structural role in controlling the enzyme activity. Moreover, replacement of this residue by an aspartate allows the enzyme to retain the catalytic activity at levels closer to those exhibited by wild type, confirming its involvement in the protonation of reaction intermediates. Our kinetic data additionally suggest that Glu^{498} is involved not only in the dioxygen reduction catalytic step(s) but also in the binding of dioxygen and presumably, of peroxide. Further research is in progress to provide more insight into the dioxygen reduction mechanism in CotA-laccase.

Ackowledgments

This work was supported by project grants from Fundação para a Ciência e Tecnologia, Portugal (POCI/BIO/57083/2004) and from European Union (BIORENEW, FP6-2004-NMP-NI-4/026456). P. Durão and Catarina S. Silva hold a Ph.D. (SFRH/BD/40696/2007 and SFRH/BD/40586/2007, respectively) and Z Chen a Post-doc fellowship (SFRH/BPD/27104/2006) from Fundação para a Ciência e Tecnologia, Portugal.

REFERENCES

1 Martins, L. O., Soares, C. M., Pereira, M. M., Teixeira, M., Costa, T., Jones, G. H. and Henriques, A. O. (2002) Molecular and biochemical characterization of a highly stable bacterial laccase that occurs as a structural component of the *Bacillus subtilis* endospore coat. J Biol Chem. **277**, 18849-18859

2 Lindley, P. (2001) Multi-copper oxidases, In Handbook on Metalloproteins (Bertini I., Siegel, A. and Sigel, H., eds) pp. 763-811, Marcel Dekker, New York

3 Messerschmidt, A. (1997) Multicopper oxidases (Messerschmidt, A, ed.) Singapore: World Scientific

4 Solomon, E. I., Sundaram, U. M. and Machonkin, T. E. (1996) Multicopper Oxidases and Oxygenases. Chem. Rev. **96**, 2563-2606

5 Stoj, C. S. and Kosman, D. J. (2005) Copper proteins: oxidases, In Encyclopedia of Inorganic Chemistry Vol II, 2nd Ed (King, R. B., ed.) pp. 1134–1159, John Wiley & Sons

6 Malmström, B. G. (1982) Enzymology of oxygen. Annu Rev Biochem. **51**, 21-59

7 Pereira, L., Coelho, A. V., Viegas, C. A., Santos, M. M., Robalo, M. P. and Martins, L. O. (2009) Enzymatic biotransformation of the azo dye Sudan Orange G with bacterial CotA-laccase. J. Biotechnol. **139**, 68-77

8 Pereira L, Coelho AV, Viegas CA, Ganachaud C, Iacazio G, Tron T, Robalo MP, Martins LO, "On the mechanism of biotransformation of the anthraquinonic dye Acid Blue 62 by laccases" Adv. Synth. Catal., 2009, DOI: 10.1002/adsc.200900271.

9 Xu, F. (1999) Laccase. In The Encyclopedia of Bioprocess Technology: Fermentation, Biocatalysis and Bioseparation (Flickinger, M.-C., Drew, S.W., ed.) pp. 1545-1554, John Wiley & Sons Inc., New York

10 Bento, I., Martins, L. O., Gato Lopes, G., Armenia Carrondo, M. and Lindley, P. F. (2005) Dioxygen reduction by multi-copper oxidases; a structural perspective. Dalton Trans, 3507-3513

11 Durão, P., Bento, I., Fernandes, A. T., Melo, E. P., Lindley, P. F. and Martins, L. O. (2006) Perturbations of the T1 copper site in the CotA laccase from *Bacillus subtilis*: structural, biochemical, enzymatic and stability studies. J. Biol. Inorg. Chem. **11**, 514-526

12 Durão, P., Chen, Z., Silva, C. S., Soares, C. M., Pereira, M. M., Todorovic, S., Hildebrandt, P., Bento, I., Lindley, P. F. and Martins, L. O. (2008) Proximal mutations at the type 1 copper site of CotA laccase: spectroscopic, redox, kinetic and structural characterization of I494A and L386A mutants. Biochem. J. **412**, 339-346

13 Enguita, F. J., Marcal, D., Martins, L. O., Grenha, R., Henriques, A. O., Lindley, P. F. and Carrondo, M. A. (2004) Substrate and dioxygen binding to the endospore coat laccase from *Bacillus subtilis*. J. Biol. Chem. **279**, 23472-23476

14 Solomon, EI, Chen, P., Metz, M., Lee, S.-K. and Palmer, A.E. (2001) Oxygen binding, activation, and reduction to water by copper proteins. Angew. Chem. Int. Ed. **40**, 4570-4590

15 Solomon, E. I., Augustine, A. J. and Yoon, J. (2008) O2 Reduction to H2O by the multicopper oxidases. Dalton Trans, 3921-3932

16 Palmer, A. E., Lee, S. K.,Solomon, E. I. (2001) Decay of the peroxide intermediate in laccase: reductive cleavage of the O-O bond. J. Am. Chem. Soc. **123**, 6591-6599

17 Machonkin, T. E., Quintanar, L., Palmer, A. E., Hassett, R., Severance, S., Kosman, D. J., Solomon, E. I. (2001) Spectroscopy and reactivity of the type 1 copper in Fet3p from *Saccharomyces cerevisae*: correlation of structure with reactivity in the multicopper oxidases. J. Am. Chem. Soc. **123**, 5507-5517

18 Palmer, A. E., Quintanar, L., Severance, S., Wang, T. P., Kosman, D. J., Solomon, E. I. (2002) Spectroscopy characterization and O2 reactivity of the trinuclear Cu cluster of mutants of the multicopper oxidase Fet3p. Biochemistry, **41**, 6438-6448
19 Hakulinen, N., Andberg, M., Kallio, J., Koivula, A., Kruus, K. and Rouvinen, J. (2008) A near atomic resolution structure of a *Melanocarpus albomyces* laccase. J Struct Biol. **162**, 29-39
20 Bento, I., Peixoto, C., Zaitsev, V. N. and Lindley, P. F. (2007) Ceruloplasmin revisited: structural and functional roles of various metal cation-binding sites. Acta Crystallogr. D Biol. Crystallogr. **63**, 240-248
21 Ducros, V., Brzozowski, A. M., Wilson, K. S., Brown, S. H., Ostergaard, P., Schneider, P., Yaver, D. S., Pedersen, A. H. and Davies, G. J. (1998) Crystal structure of the type-2 Cu depleted laccase from *Coprinus cinereus* at 2.2 A resolution. Nat. Struct. Biol. **5**, 310-316.
22 Ferraroni, M., Myasoedova, N. M., Schmatchenko, V., Leontievsky, A. A., Golovleva, L. A., Scozzafava, A. and Briganti, F. (2007) Crystal structure of a blue laccase from *Lentinus tigrinus*: evidences for intermediates in the molecular oxygen reductive splitting by multicopper oxidases. BMC Struct. Biol. **7**, 60
23 Garavaglia, S., Cambria, M. T., Miglio, M., Ragusa, S., Iacobazzi, V., Palmieri, F., D'Ambrosio, C., Scaloni, A. and Rizzi, M. (2004) The structure of *Rigidoporus lignosus* Laccase containing a full complement of copper ions, reveals an asymmetrical arrangement for the T3 copper pair. J. Mol. Biol. **342**, 1519-1531
24 Li, X., Wei, Z., Zhang, M., Peng, X., Yu, G., Teng, M. and Gong, W. (2007) Crystal structures of *E. coli* laccase CueO at different copper concentrations. Biochem. Biophys. Res. Commun. **354**, 21-26
25 Lyashenko, A. V., Bento, I., Zaitsev, V. N., Zhukhlistova, N. E., Zhukova, Y. N., Gabdoulkhakov, A. G., Morgunova, E. Y., Voelter, W., Kachalova, G. S., Stepanova, E. V., Koroleva, O. V., Lamzin, V. S., Tishkov, V. I., Betzel, C., Lindley, P. F. and Mikhailov, A. M. (2006) X-ray structural studies of the fungal laccase from *Cerrena maxima*. J. Biol. Inorg. Chem. **11**, 963-973
26 Messerschmidt, A., Ladenstein, R., Huber, R., Bolognesi, M., Avigliano, L., Petruzzelli, R., Rossi, A. and Finazzi-Agro, A. (1992) Refined crystal structure of ascorbate oxidase at 1.9 A resolution. J. Mol. Biol. **224**, 179-205.
27 Piontek, K., Antorini, M. and Choinowski, T. (2002) Crystal structure of a laccase from the fungus *Trametes versicolor* at 1.90-A resolution containing a full complement of coppers. J. Biol. Chem. **277**, 37663-37669
28 Taylor, A. B., Stoj, C. S., Ziegler, L., Kosman, D. J. and Hart, P. J. (2005) The copper-iron connection in biology: structure of the metallo-oxidase Fet3p. Proc. Natl. Acad. Sci. U S A. **102**, 15459-15464
29 Augustine, A. J., Quintanar, L., Stoj, C. S., Kosman, D. J. and Solomon, E. I. (2007) Spectroscopic and kinetic studies of perturbed trinuclear copper clusters: the role of protons in reductive cleavage of the O-O bond in the multicopper oxidase Fet3p. J. Am. Chem. Soc. **129**, 13118-13126
30 Kataoka, K., Kitagawa, R., Inoue, M., Naruse, D., Sakurai, T. and Huang, H. W. (2005) Point mutations at the type I Cu ligands, Cys457 and Met467, and at the putative proton donor, Asp105, in *Myrothecium verrucaria* bilirubin oxidase and reactions with dioxygen. Biochemistry. **44**, 7004-7012
31 Kataoka, K., Sugiyama, R., Hirota, S., Inoue, M., Urata, K., Minagawa, Y., Seo, D. and Sakurai, T. (2009) Four-electron Reduction of Dioxygen by a Multicopper Oxidase, CueO, and

Roles of Asp(112) and Glu(506) Located Adjacent to the Trinuclear Copper Centre. J. Biol. Chem. **284**, 14405-14413
32 Quintanar, L., Stoj, C., Wang, T. P., Kosman, D. J. and Solomon, E. J. (2005) Role of aspartate 94 in the decay of the peroxide intermediate in the multicopper oxidase Fet3p. Biochemistry. **44**, 6081-6091
33 Ueki, Y., Inoue, M., Kurose, S., Kataoka, K. and Sakurai, T. (2006) Mutations at Asp112 adjacent to the trinuclear Cu centre in CueO as the proton donor in the four-electron reduction of dioxygen. FEBS Lett. **580**, 4069-4072
34 Durao, P., Chen, Z., Fernandes, A. T., Hildebrandt, P., Murgida, D. H., Todorovic, S., Pereira, M. M., Melo, E. P. and Martins, L. O. (2008) Copper incorporation into recombinant CotA laccase from Bacillus subtilis: characterization of fully copper loaded enzymes. J. Biol. Inorg. Chem. **13**, 183-193
35 Aasa, R. and Väangard, V. T. (1975) EPR Signal Intensity and Powder Shapes - Re-Examination. J. Magnet. Reson. **19**, 308-315
36 Bradford, M. M. (1976) Rapid and Sensitive Method for Quantitation of Microgram Quantities of Protein Utilizing Principle of Protein-Dye Binding. Anal. Biochem. **72**, 248-254
37 Leslie, A. G. (2006) The integration of macromolecular diffraction data. Acta Crystallogr D Biol Crystallogr. **62**, 48-57
38 CCP4 (1994) Collaborative computational project. Number 4. Acta Crystallogr. Sect. D Biol Crystallogr. **50**, 760-763
39 Vagin, A. and Teplyakov, A. (1997) MOLREP: an automated program for molecular replacement. J. Appl. Crystallogr. **30**, 1022-1025
40 Murshudov, G. N., Vagin, A. A. and Dodson, E. J. (1997) Refinement of macromolecular structures by the maximum-likelihood method. Acta Crystallogr D Biol Crystallogr. **53**, 240-255
41 Emsley, P. and Cowtan, K. (2004) Coot: model-building tools for molecular graphics. Acta Crystallogr D Biol Crystallogr **60**, 2126-2132
42 Xu, F. (2001) Dioxygen reactivity of laccase - Dependence of laccase source, pH, and anion inhibition. Appl. Biochem. Biotechnol. **95**, 125-133
43 Kataoka, K., Sugiyama, R., Hirota, S., Inoue, M., Urata, K., Minagawa, Y., Seo, D. and Sakurai, T. (2009) Four-electron Reduction of Dioxygen by a Multicopper Oxidase, CueO, and Roles of Asp(112) and Glu(506) Located Adjacent to the Trinuclear Copper Center. J. Biol. Chem. **284**, 14405-14413

FIGURE LEGENDS

Figure 1 Structural detail of the trinuclear Cu site in the native CotA laccase structure showing the Glu^{498} residue that forms a hydrogen bond with a water molecule in the access solvent channel to the trinuclear centre that in turn is hydrogen bonded to dioxygen.

Figure 2 pH profile for catalytic activities using as substrates ABTS (A) and 2,6-DMP (B). Wild-type (circle) and E498L (square), E498T (triangle) and E498D mutants (diamonds).

Figure 3 UV-visible absorbance spectra of wild-type (thick line), and CotA mutants: E498L (thin line), E498T (semi-dot line) and E498D (dotted line). Proteins were treated with the oxidizing agent potassium iridate.

Figure 4 EPR spectra of the wild-type (A), E498L (B), E498T (C) and E498D (D), obtained at 10 K and microwave frequency, 9.39 GHz; power, 2.0 mW; modulation amplitude: 0.9 mT. The spectra were simulated using the spin Hamiltonian parameters presented in table 4.

Figure 5 Structural detail of the trinuclear centre and its neighbourhood in CotA a), in E498D b), in E498T c) and in E4098L mutants.

Supplementary material

Figure S1 Experimental and deconvoluted RR spectra of wild-type CotA (A), E498L (B), E498T (C) and E498D (D) mutants obtained with 568 nm excitation and 5mW laser power at 77K, accumulation time 40s.

Table 1 X-ray data collection

	E498D	E498T	E498L
Beam line at ESRF	ID23-2	ID14-1	ID14-1
Wavelength (Å)	0.8726	0.934	0.934
Detector Distance (mm)	223.2	193.3	162.0
Resolution (Å)	2.1	2.0	1.7
Space group	$P3_12_1$	$P3_12_1$	$P3_12_1$
Cell parameters (Å), a	101.83	101.90	101.57
C	136.57	136.93	136.29
Mosaicity (^{o})	0.85	0.66	0.50
Oscillation range (^{o})	1.0	0.5	1.0
Oscillation angle (^{o})	65^o	60^o	60^o
No. of unique *hkl*	48362 (7000)	55879 (8055)	89089 (12978)
Completeness (%)	99.9 (100.0)	99.6 (99.7)	99.5 (100.0)
I/σ(I)	6.6 (2.0)	9.2 (2.2)	10.4 (2.4)
R_{symm}	0.083 (0.37)	0.069 (0.348)	0.053 (0.321)
Multiplicity	4.0 (4.0)	5.1 (3.6)	5.5 (4.6)

† Values in parentheses refer to the highest resolution shells as follows;

E498D (2.21Å - 2.10 Å)

E498T (2.11 Å - 2.00 Å)

E498L (1.79 Å - 1.70 Å)

Table 2 Apparent steady-state kinetic constants for ABTS and 2,6-DMP by the CotA proteins measured at saturating concentrations of O_2

CotA	ABTS			2,6-DMP		
	K_m (μM)	k_{cat} (s^{-1})	k_{cat}/K_m ($s^{-1}\mu M^{-1}$)	K_m (μM)	k_{cat} (s^{-1})	k_{cat}/K_m ($s^{-1}\mu M^{-1}$)
Wild type	110 ± 14	251 ± 30	2.3	227 ± 41	36 ± 5	0.16
E498D	61 ± 28	16 ± 2	2.6×10^{-1}	208 ± 46	1.3 ± 0.6	0.6×10^{-2}
E498T	120 ± 12	1.7 ± 0.6	1.4×10^{-2}	137 ± 28	0.05 ± 0.03	0.4×10^{-3}
E498L	106 ± 10	0.09 ± 0.03	0.6×10^{-3}	180 ± 4	0.006 ± 0.004	0.3×10^{-4}

Table 3 $K_{m\ app}(O_2)$ of wild-type and mutants measured with 1mM of ABTS and I_{50} after a 30 minutes incubation period with sodium azide (similar values were obtained after 60 and 120 min of incubation)

CotA	$K_{m\ app}(O_2)$ (μM)	Azide I_{50} (mM)
Wild type	25 ± 13	2.3 ± 0.0
E498D	19 ± 13	2.3 ± 0.0
E498T	58 ± 15	4.7 ± 0.2
E498L	92 ± 10	9.8 ± 0.1

Table 4 EPR parameters used in the simulation of wild-type and CotA mutants spectra

CotA	Cu centres	contribution	g_{min}	g_{med}	g_{max}	A_{max} (x 10^{-4} cm^{-1})
Wild type	T1	1	2.042	2.046	2.228	78
	T2	1	2.035	2.094	2.250	195
E498D	T1	0.5	2.042	2.047	2.230	78
	T2	1	2.035	2.094	2.245	210
	T2’	1	2.035	2.094	2.330	110
E498T	T1	1	2.042	2.046	2.235	75
	T2	1	2.035	2.094	2.325	124
E498L	T1	1	2.042	2.046	2.225	78
	T2	1	2.035	2.090	2.250	190

SUPPLEMENTARY MATERIAL

Table S1 Refinement and quality of refined models. The Ramachandran analysis [1] was determined by Rampage [2]

	E498D	E498T	E498L
No. of protein atoms	4122	4119	4150
No. of solvent atoms	495	518	645
No. of hetero atoms	4	4	4
Final R-factor	0.177	0.177	0.175
Final free R-factor	0.206	0.215	0.194
Mean B values (Å^2)			
: protein	26.04	24.25	17.65
: solvent	36.91	32.94	30.69
: overall	27.25	25.26	19.47
Estimated overall coordinate uncertainty (´) ‡	0.088	0.089	0.049
Distance deviations †			
Bond distances (´)	0.007	0.009	0.007
Bond angles (^{o})	1.036	1.145	1.064
Planar groups (´)	0.003	0.004	0.003
Chiral volume deviation (´^{3})	0.068	0.077	0.071
Quality of Models*			
Ramachandran analysis %			
Favourable	97.2	97.8	97.2
Allowed	2.8	2.2	2.8
Disallowed	0.0	0.0	0.0

‡ based on maximum likelihood.
† rms deviations from standard values

1 Ramakrishnan C. and Ramachan,G. N. (1965) Stereochemical criteria for polypeptide and protein chain conformations. Biophys. J. **5**, 909-933

2 Lovell, S. C., Davis, I. W., Adrendall, W. B., de Bakker, P. I. W., Word, J. M., Prisant, M. G., Richardson, J. S. and Richardson, D. C. (2003) Structure validation by C alpha geometry: phi,psi and C beta deviation. Proteins-Structure Function and Genetics. **50**, 437-450

Table S2 Copper content, molar absorptivity, and reduction potentials for CotA proteins

CotA	Copper content	E^o	ε_{330} nm as-isolated	ε_{330} nm oxidized	ε_{609} nm as isolated	ε_{609} nm oxidized
	g atoms Cu/mol CotA	*mV*	$mM^{-1}.cm^{-1}$	$mM^{-1}.cm^{-1}$	$mM^{-1}.cm^{-1}$	$mM^{-1}.cm^{-1}$
Wild type	4.2 ± 0.1	525	3.4 ± 0.1	4.4 ± 0.8	3.8 ± 0.3	3.9 ± 0.4
E498D	3.7 ± 0.2	525	1.0 ± 0.02	3.1 ± 0.3	1.3 ± 0.02	1.6 ± 0.1
E498T	3.7 ± 0.1	521	1.8 ± 0.2	3.3 ± 0.9	3.2 ± 0.7	3.4 ± 0.7
E498L	3.7 ± 0.2	516	1.6 ± 0.1	3.7 ± 0.2	0.8 ± 0.1	3.4 ± 0.1

Table S3 Occupancies of copper sites in the crystal structures

CotA / Copper Site	Wild type	E498T	E498L	E498D
Type 1	1.0	1.0	1.0	0.7
Type 2	1.0	0.8	0.3	1.0
Type 3 (x2)	1.0	0.8	0.8	1.0

Chen et al Figure 1

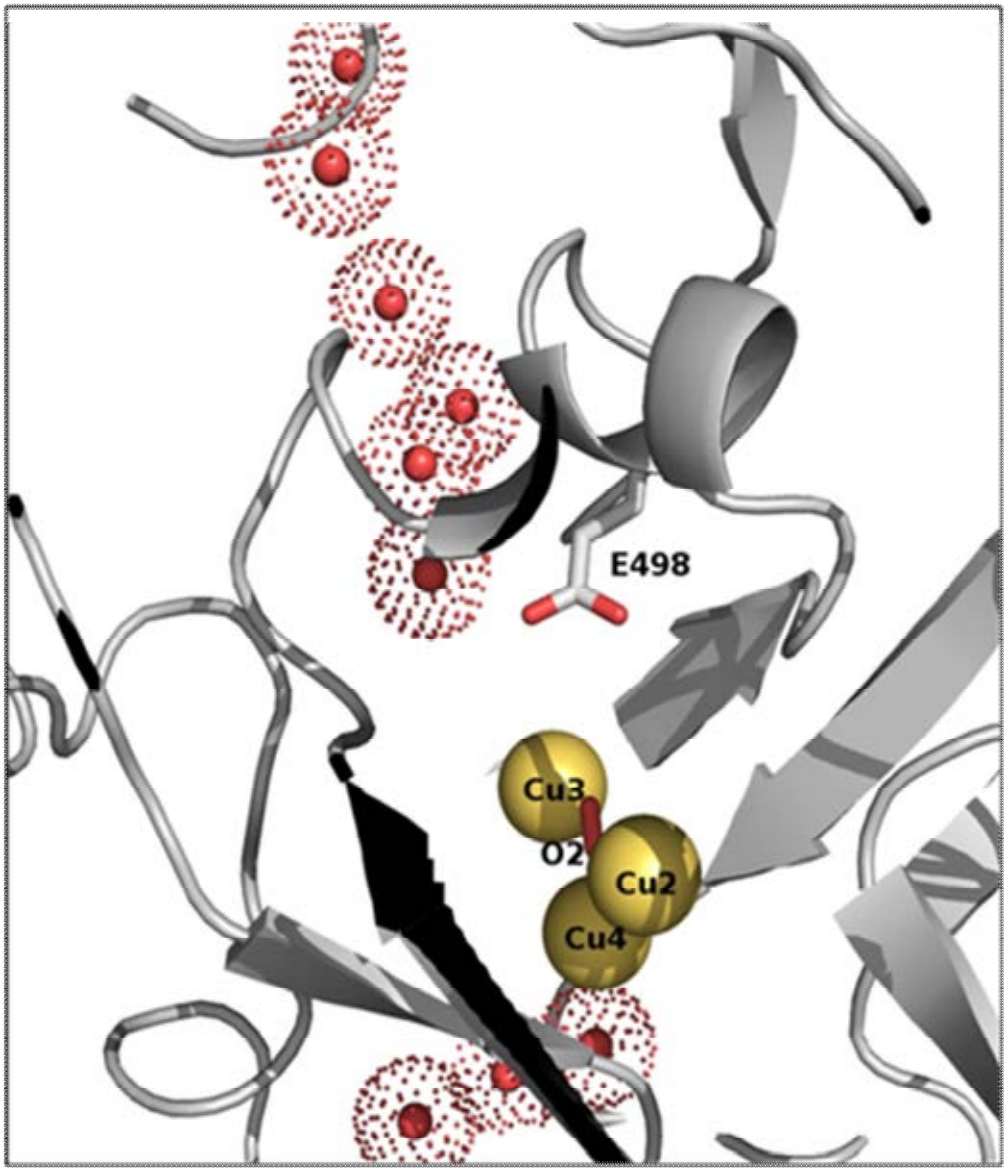

Chen et al

Figure 2

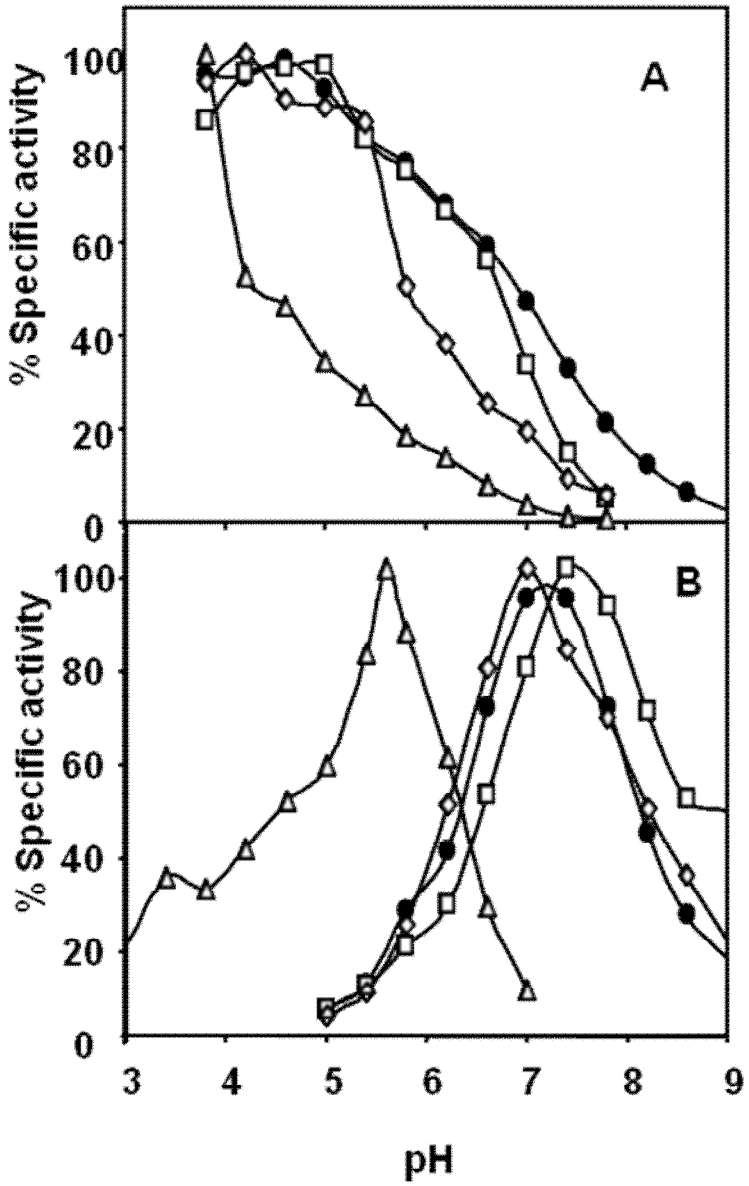

Chen et al

Figure 3

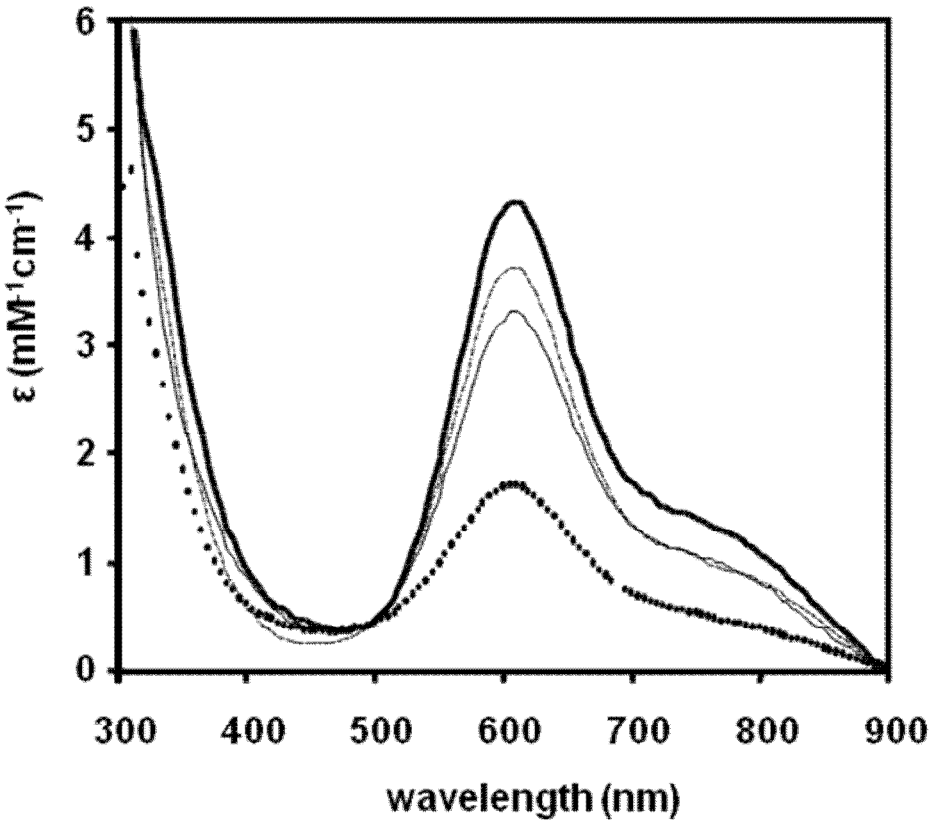

Chen et al

Figure 4

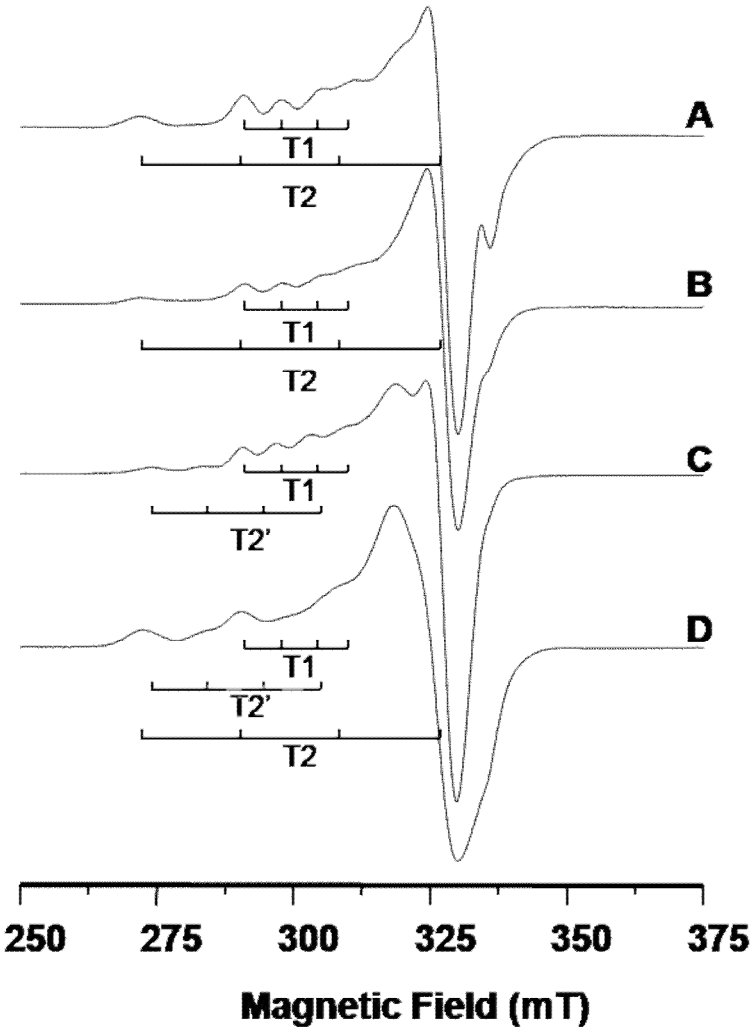

Chen et al

Figure 5

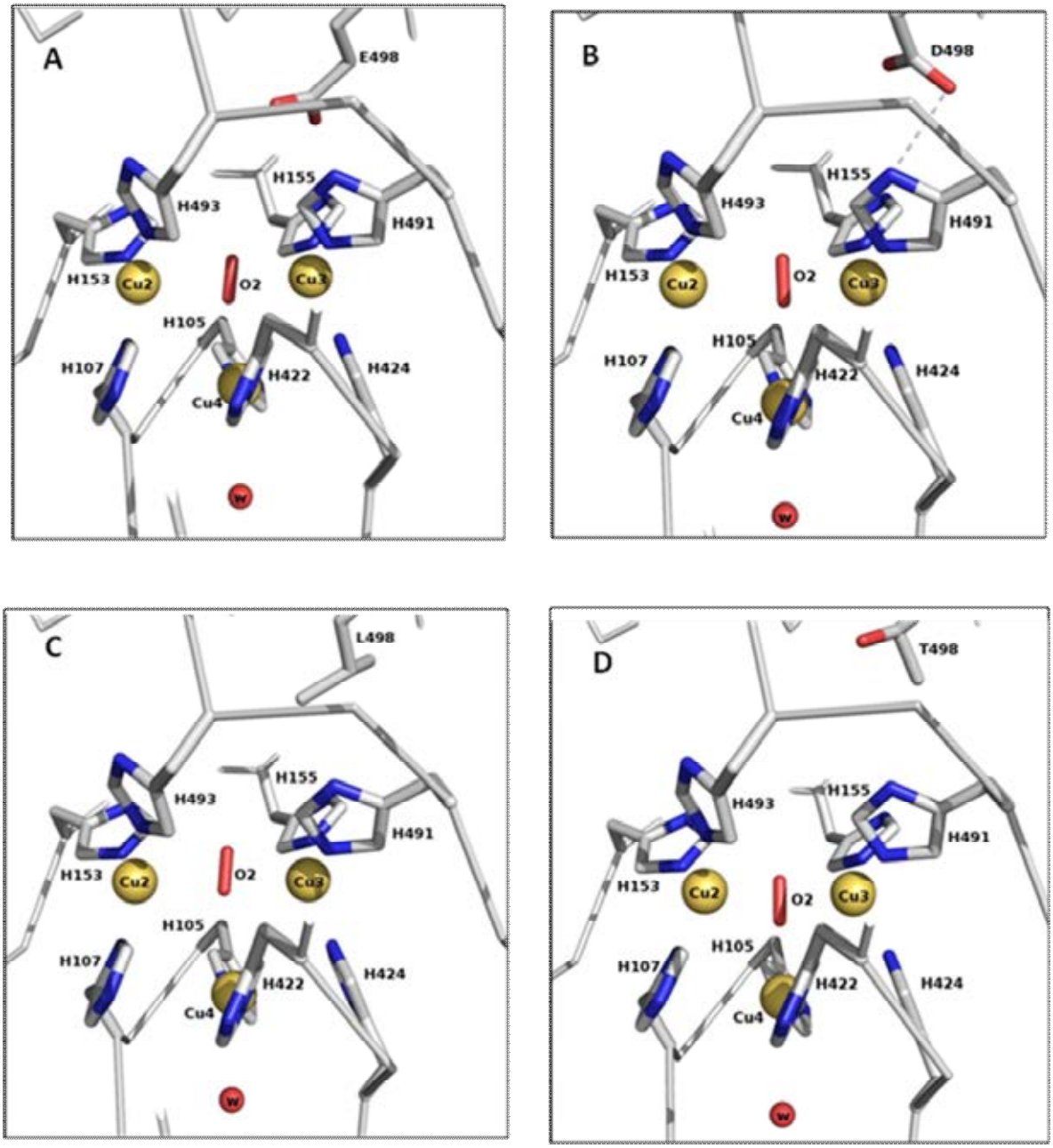

Chen et al **Figure S1**